Anisotropic angular distribution of fragment ions in dissociative double photoionization of OCS

Toshio Masuoka
Department of Applied Physics, Osaka City University, Sumiyoshi-ku, Osaka 558, Japan

Inosuke Koyano
Department of Material Science, Himeji Institute of Technology, Kamigori-cho, Ako-gun, Hyogo 678-12, Japan

Norio Saito
Electrotechnical Laboratory, Umezono, Tsukuba-shi, Ibaraki 305, Japan
(Received 16 May 1991)

Angular distributions of fragment ions produced in the dissociative double photoionization of OCS have been studied in the photon energy region 37–100 eV with the use of synchrotron radiation and photoion-photoion coincidence. The asymmetry parameter β ranges from 0.01 to 0.48 for the three major dissociation channels $OC^+ + S^+$, $O^+ + S^+ + C$, and $C^+ + S^+ + O$ of OCS^{2+}. The observation of an anisotropy in the direct double photoionization from valence orbitals is discussed in relation to the symmetry consideration involved in the transition and the dynamics of the dissociation.

PACS number(s): 33.80.Eh, 33.80.Gj, 33.90.+h

I. INTRODUCTION

It has been widely recognized that the angular distributions of neutral fragments produced in molecular photodissociation are closely related to the symmetry and dynamics of the processes involved [1]. If a dipole-allowed Σ-Σ or Π-Π transition occurs in randomly oriented linear molecules or ones with cylindrical symmetry by absorption of linearly polarized light ($\Delta\Lambda=0$, the transition moment is parallel to the molecular axis), then the form of the anisotropy is $\cos^2\theta$ (parallel transition). If a Σ-Π or Π-Δ transition occurs ($\Delta\Lambda=\pm1$, the transition moment is perpendicular to the molecular axis), then the form of the anisotropy is $\sin^2\theta$ (perpendicular transition) under axial recoil conditions, i.e., the decay time is small enough compared to one rotational period. The angle θ is measured relative to the direction of the electric vector of the light. In the case of dissociative photoionization, the angular distribution of a given fragment ion depends on the symmetry of the total final state (i.e., molecular ion plus photoelectron), following the same formalism mentioned above as studied for H_2 at 40.8 eV [2], and also in the region of the K-shell excitation and ionization for N_2 [3,4], O_2 [5], and NO [6]. Very recently, anisotropy of the CF_2I^+ and I^+ fragment ions has been recorded in the region of the CF_3I^+ A state [7].

Although similar types of symmetry-characterized dissociation may also occur in direct double ionization (not via Auger decay), anisotropy of fragment ions has not been detected as yet for two-body dissociation by photoion-photoion coincidence (PIPICO) spectroscopy [8–11]. For three-body dissociation, Eland has observed angular correlations among the three fragments ($A^+ + B^+ + C$ from ABC^{2+}) by a triple coincidence photoelectron PIPICO (PEPIPICO) experiment [12] but no detailed modeling or symmetry consideration was given for the angular correlations.

We have recently studied the dissociative single, double, and triple photoionization in the valence region of OCS [13] and some other molecules [Al $(CH_3)_3$ (Ref. [14]) and SiF_4 (Ref. [15])] using synchrotron radiation, time-of-flight mass spectrometry, and PIPICO spectroscopy. In the present work on OCS we report an observation of the anisotropic angular distribution of fragment ions in direct dissociative double photoionization. Kinetic energies released in the observed dissociation channels will be reported separately [16].

II. EXPERIMENT

The PIPICO spectra were measured by use of synchrotron radiation and a time-of-flight (TOF) mass spectrometer [13,17]. In the PIPICO measurements, two ions that were produced as a pair in the dissociative double photoionization were drawn into the 20-cm-long TOF drift tube, and the ion signal was fed into both the start and stop inputs of the time-to-amplitude converter (TAC). The TOF difference between the lighter and heavier ions was then determined on the multichannel analyzer and read out into a microcomputer. A relatively high electric field ($\sim$600 V/cm) was applied to the ionization chamber, which had a 6-mm-diam hole for ion extraction. The entrance aperture of the drift tube was 8 mm in diameter. A constant-deviation grazing-incidence monochromator [18], installed at the UVSOR synchrotron-radiation facility in Okazaki, and an optical filter (Al+Te, 37–58 eV; Be, 59–69 eV; no filter above 69 eV) provided monochromatic radiation. The bandpass of the monochromator was about 0.8 or 1.6 Å with a 400-μm-wide entrance and exit slits when a blazed holographic grating of 2400 lines/mm (above 59 eV) or 1200 lines/mm (32–58 eV), respectively was used. The accepted angular divergence of the photon beam was $\sim$5 (vertical)$\times$10 (horizontal) mrad^2. Five mirrors and one grat-

ing were set on the beam line. Since two of those reflected the beam horizontally and the other four vertically, the degree of polarization (p) was likely to be relatively high ($p=0.9$ was assumed in the analysis). The value p of synchrotron radiation emitted from a storage ring (750 MeV) prior to the six optical reflections in the beamline is calculated to be 0.58 at 42.5 eV and 0.65 at 127.6 eV, which gives a lower limit to the polarization applicable to the experiment.

The TOF mass spectrometer could be rotated through 90° around the photon beam in order to measure the characteristic profiles of PIPICO peaks. In most cases the ion detection axis was set at 55°, 0°, or 90°, the latter two being parallel or perpendicular, respectively, to the electric vector of the incident polarized light, and in some cases at 35°. The sample gas pressure in the ionization chamber was not directly measured during the measurements and was maintained so as to keep the background pressure in the main chamber at about 5×10^{-7} Torr.

III. ANALYSIS OF PIPICO SPECTRA

A typical PIPICO spectrum measured at $h\nu=80$ eV and $\theta=55°$ (Fig. 1) shows five dissociation channels of OCS^{2+}, i.e., $OC^+ + S^+$, $C^+ + O^+ + S$, $O^+ + S^+ + C$, $C^+ + S^+ + O$, and $O^+ + CS^+$, and one dissociation channel of OCS^{3+}, i.e., $OC^+ + S^{2+}$ [13]. The asymmetry parameter β was obtained for the three major dissociation channels $OC^+ + S^+$ (37–50 eV), $O^+ + S^+ + C$ (50–100 eV), and $C^+ + S^+ + O$ (45–100 eV) in the energy regions indicated in brackets and for the channel $O^+ + CS^+$ at 50 eV. The threshold of these four channels lies at 33.5, 45, 40, and 40 eV, respectively [13]. Although it is highly desirable to obtain an asymmetry parameter of the channel $OC^+ + S^+$ slightly above the dissociation threshold (33.5 eV), where the electronic states of OCS^{2+} responsible for that channel are well defined [19], PIPICO signals were too weak to exhibit a reliable spectral profile within a reasonable data-acquisition time. This is because the use of an optical filter Sn, which is necessary below 37 eV for order sorting, reduced the light intensity more than two orders of magnitude. The dissociation channel $OC^+ + S^+$ was analyzed only up to 50 eV because the channel $C^+ + O^+ + S$ overlapped above this energy.

When the TOF spectrometer is rotated in a plane perpendicular to the light beam, the differential partial cross section for the partially polarized light is given by

$$\frac{\partial\sigma_i}{\partial\Omega}=\frac{\sigma_i}{4\pi}\left[1+\frac{\beta}{4}(3p\cos2\theta+1)\right], \tag{1}$$

where p is the degree of polarization given by

$$p=\frac{I_\parallel-I_\perp}{I_\parallel+I_\perp}, \tag{2}$$

β is the asymmetry parameter that characterizes the angular distribution, θ is the angle of the PIPICO spectrometer axis relative to the electric vector of the light, and I is the incident light intensity [2,20]. The degree of polarization has not been measured and in the analysis of the PIPICO spectra we assume $p=0.9$ for the reason mentioned in Sec. II. Depending on whether the transition moment is parallel or perpendicular to the molecular axis (dissociation axis), the angular distribution is given by $\cos^2\theta$ ($\beta=2$) or $\sin^2\theta$ ($\beta=-1$), respectively, under the axial recoil conditions. Characteristic features of the simulated spectral profiles are summarized in Fig. 2 for the simple case that the fragment ions have a single-

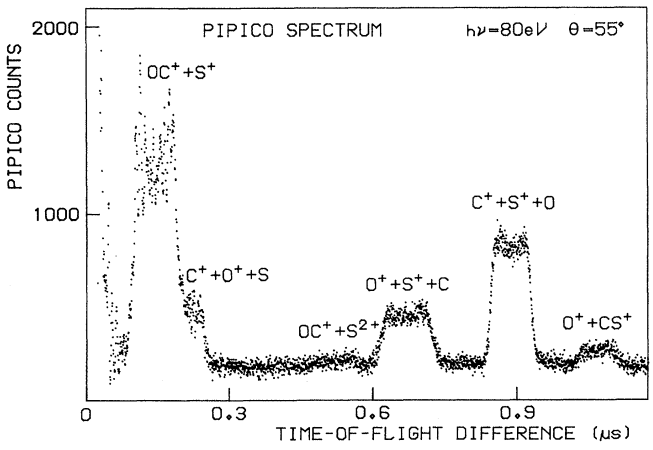

FIG. 1. PIPICO spectrum measured at $h\nu=80$ eV and $\theta=55°$. Five dissociation channels of OCS^{2+} and one of OCS^{3+} can be seen. Superimposed on the spectrum in the shorter time range are accidental coincidences that reflect the time structure of the storage ring (Ref. [13]).

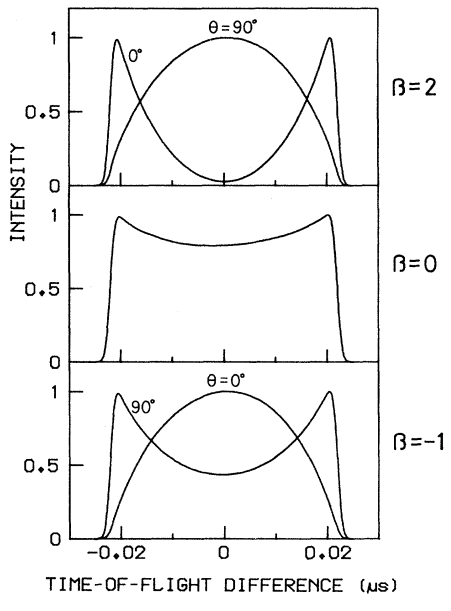

FIG. 2. Simulated PIPICO spectral profiles of fragment ions with a single-valued kinetic energy at $\theta=0°$ and 90° with respect to the ion detection axis for parallel ($\beta=2$), isotropic ($\beta=0$), and perpendicular ($\beta=-1$) transitions. The profiles show characteristic features of anisotropic angular distributions. The channel $C^+ + S^+ + O$ and the total kinetic energy of 10 eV for $C^+ + S^+$ were assumed. Other conditions are the same as the experimental ones.

valued kinetic energy. As can be seen clearly in the figure, the spectral profile is a good measure of anisotropic angular distributions.

The spectral profiles of PIPICO peaks are determined by the kinetic-energy distribution and the angular distribution of the fragment ions, both with respect to the spectrometer axis, and other experimental conditions such as the electric field across the ionization region, the size and the degree of polarization of the photon beam, and so on. In order to obtain the angular distribution of the fragment ions, it is first necessary to determine the kinetic-energy distribution of the ionic fragments without any effects of the angular distribution. As can be seen from Eq. (1), the differential partial cross section is independent of the asymmetry parameter if $3p\cos2\theta+1=0$ [$\theta=\frac{1}{2}\arccos(-1/3p)$]. For this reason, the kinetic-energy distributions were obtained by analyzing the PIPICO spectra measured at the so-called "pseudomagic angle," which is equal to about 55° under the assumed condition that $p=0.9$.

The analysis of the spectral profiles of PIPICO peaks uses a least-squares fit of the simulated profiles to those measured, and has been described elsewhere in detail [21]. The following were assumed in the simulation of the spectral profiles. (1) The cross section of the photon beam is elliptical with a size of 2 mm wide and 1.5 mm high (maximum) over which the light intensity is constant. (2) Both the gas density and the formation of ions are uniform along the photon beam in the ionization region where there is no magnetic field and the electric field is exactly the same as that intended. (3) Two ionic fragments depart in the opposite direction with the same momentum in the fragmentation and the neutral fragment produced in three-body dissociation (e.g., $OCS^{2+}\rightarrow C^{+}+S^{+}+O$) does not have any appreciable kinetic energy. This assumption is correct for only a limited case of the possible dissociation mechanisms and will be discussed later. (4) The spectral profiles of PIPICO peaks do not depend on the anisotropy of fragment ions for measurements at the pseudomagic angle. (5) Although the real kinetic-energy distribution is continuous, the observed spectral profile can be reproduced well by superposition of simulated profiles for a set of several discrete kinetic energies (W_i) by choosing their weighting coefficients properly.

The following is a brief summary of the method to calculate the spectral profile of a PIPICO peak for a given kinetic energy. We note that an ion pair, one departing at an angle α relative to the spectrometer axis and the other in the opposite direction, has the same TOF difference irrespective of the departing azimuthal angle and the initial position of the ion pair, so that the spectral profile of the PIPICO peak is determined by the ion flux intensity detected as a function of the departing angle α. From an ion trajectory calculation (the details have been given in Ref. [21]), the fraction of ion pairs that went through the aperture of the ion chamber and reached the ion detector was determined for a given initial position of the ion pair. Then the ion intensity of a given TOF difference corresponding to the angle α was given by a numerical integration of the calculated fraction over the ionization region. Finally the spectral profile of the PIPICO peak was obtained by calculating the ion intensity for an appropriate interval of the angle α, i.e., an interval of the TOF difference.

The kinetic energy W_i in the simulation was chosen so as to keep the difference $(W_i)^{1/2}-(W_{i-1})^{1/2}$ constant because the time-of-flight difference in a PIPICO peak is proportional to the square root of the kinetic energy. Then the total width of a simulated profile for each kinetic energy increases with a constant interval. The spectral profile calculated for isotropically dissociated ($\beta=0$) fragment ions with kinetic energy W_i was convoluted with a Gaussian distribution of proper width. This broadening of the spectral profile by a Gaussian distribution and the choice of W_i noted above were necessary to obtain a smooth fit. Let the spectral profile thus calculated be $F(W_i)$. The observed spectral profile $S(t)$ is given by

$$S(t)=\sum_i c_i F(W_i)\ . \tag{3}$$

The coefficient c_i was determined by a least-squares fit to the observed spectral profile. Then the kinetic-energy distribution per unit energy is given by plotting $c_i/\eta_i/[(W_{i+1}-W_{i-1})/2]$ vs W_i, where η_i is the collection efficiency of the PIPICO spectrometer for the fragment ions with kinetic energy W_i.

The procedure for determining the β parameter is as follows. (1) Spectral profiles at an angle θ (typically 0° and 90°) were calculated for a set of various kinetic energies of the fragment ions with an arbitrarily fixed β parameter. (2) The spectral profile of the PIPICO peak at the angle θ was calculated, based on the kinetic-energy distribution already determined and the profiles calculated in step 1. (3) By treating the β value as a running parameter, its most probable value was determined as the one for which the sum of squares of the residuals between the observed and calculated profiles was minimized.

IV. RESULTS AND DISCUSSION

Shown in Fig. 3 are two typical examples of observed spectral profiles: one for the $OC^{+}+S^{+}$ channel at $h\nu=45$ eV in (a) and the other for the $C^{+}+S^{+}+O$ channel at 80 eV in (b), both measured at $\theta=55°$. The simulated spectral profiles are also shown in the figure. The total mean kinetic energy of 5.4 eV is obtained for $OC^{+}+S^{+}$, which compares well with 5.3 eV measured with He II light (not dispersed) [12] or 5.4 eV measured at 43.5 eV [22]. For the three-body dissociation $C^{+}+S^{+}+O$, the mean kinetic energy involved in the two ionic fragments in the direction parallel to the PIPICO spectrometer axis is 8.0 eV. In this case, the presence of the neutral adds uncertainty to the determination of kinetic energy spread and asymmetry parameter. If the neutral is a spectator, the results derived in the present study for both parameters are well defined and acceptable. On the other hand, if the neutral participates, the kinetic energy will be bigger and the asymmetry parameters that are derived give only a rough measure. Information on the dynamics of the three-body dissociation has been provided by the triple coincidence technique

(PEPIPICO) [12]. For the $C^+ + S^+ + O$ channel, the O atom is a spectator. However, a small deviation from the linear dissociation has been observed for the $O^+ + S^+ + C$ channel of OCS^{2+} formed by 40.8–48-eV photons [12].

Figure 4 shows the spectral profiles of the $OC^+ + S^+$ peak measured at 45 eV and $\theta = 0°$ and 90°. Both profiles are different from the one in Fig. 3(a). This is clear evidence of anisotropy in this channel. The simulated profiles are those for $\beta = 0.35$ for which the best fit was attained. The asymmetry parameters for the channel $OC^+ + S^+$ are shown in Fig. 5, where the value ranges from 0.1 (at 37 eV) to 0.37 (the mean at 50 eV) in the photon energy region of 37–50 eV. The scatter of the data points measured at different angles gives a rough measure of uncertainty. Furthermore, if the degree of polarization is different by ± 0.1 from the assumed one ($p = 0.9$), the uncertainly in β becomes slightly larger than that given by the scatter of the data points.

Now we discuss the observed asymmetry parameters. The valence shell electronic configuration of OCS in the ground electronic state is

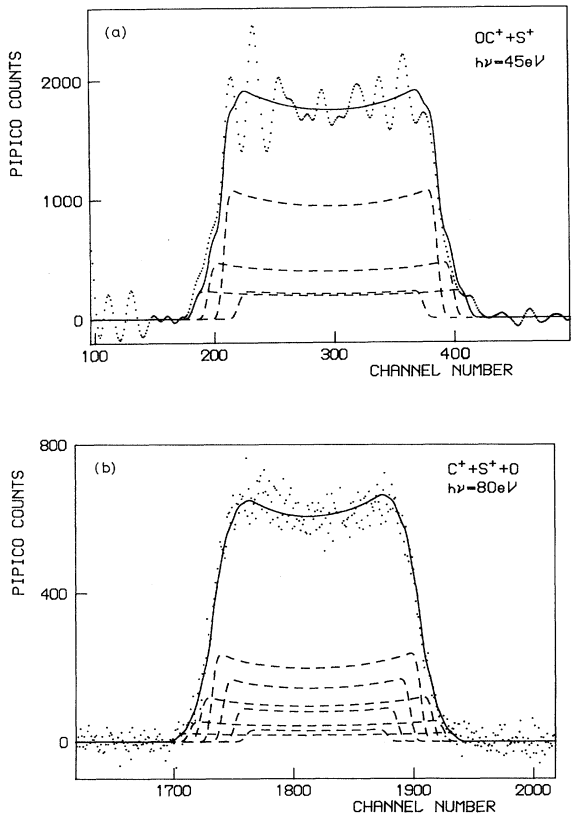

FIG. 3. (a) Observed (dots; five-point average of the original data) and simulated (solid line) spectral profiles of $OC^+ + S^+$ at $h\lambda = 45$ eV and $\theta = 55°$ (simulated profiles for the set of kinetic energies W_i of 3.6, 4.8, 6.2, and 7.8 eV from inside to outside are shown by dashed lines) and (b) those of $C^+ + S^+ + O$ at $h\lambda = 80$ eV and $\theta = 55°$ (kinetic energies W_i of 3.6, 4.8, 6.2, 7.8, 9.6, 11.6, and 13.7 eV from inside to outside were assumed). Superimposed on the observed spectrum in (a) are accidental coincidences that reflect the time structure of the storage ring (Ref. [13]).

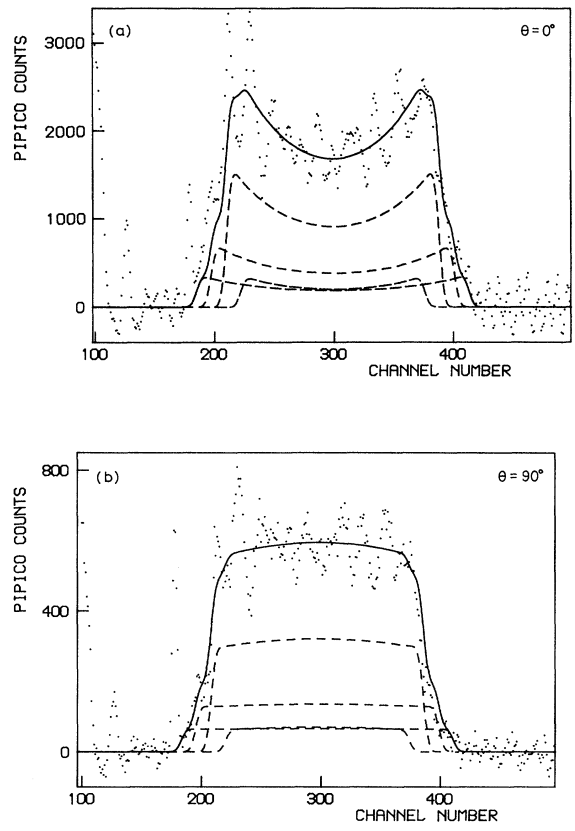

FIG. 4. Observed (dots) and simulated (solid line) spectral profiles indicating clear evidence of anisotropy in the channel $OC^+ + S^+$ at $h\lambda = 45$ eV. (a) $\theta = 0°$ and (b) $\theta = 90°$; both give $\beta = 0.35$. The same set of kinetic energies assumed for Fig. 3(a) was used for the dashed lines.

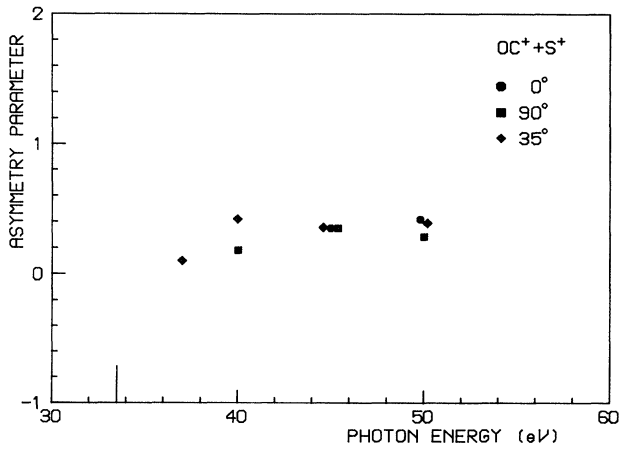

FIG. 5. Asymmetry parameter β for the channel $OC^+ + S^+$ measured at $\theta = 0°$ (●), 90° (■), and 35° (◆) in the energy region 37–50 eV. The vertical bar indicates the dissociation threshold for the channel $OC^+ + S^+$ at 33.5 eV.

$$(\text{core})^{14}(6\sigma)^2(7\sigma)^2(8\sigma)^2(9\sigma)^2(2\pi)^4(3\pi)^4:{}^1\Sigma^+$$

in the independent-particle description with a geometric symmetry of $C_{\infty v}$. In the two-electron ejection

$$\langle n_1\lambda_1|\mathbf{r}|\epsilon_1\lambda_1'\rangle\langle n_2\lambda_2|\epsilon_2\lambda_2'\rangle ,$$

the selection rules are $\lambda_1'=\lambda_1,\pm1$ (which we call dipole allowed for convenience), and $\lambda_2'=\lambda_2$ (overlap allowed), where n is the principal quantum number, λ is the orbital angular momentum, and ϵ represents the continuum channel. The symmetry of the doubly charged ionic states, the dipole- and overlap-allowed photoelectron symmetry, and the total symmetry (doubly charged ion plus two photoelectrons) are listed in Table I for the possible electron configurations of OCS^{2+}.

According to a theoretical calculation [19], the accessible states of OCS^{2+} at the photon energy of 37 eV (6 eV above the appearance potential of OCS^{2+} at 31.0 eV [13] and 3.5 eV above the dissociation threshold at 33.5 eV [19]) are those arising from the configurations $3\pi^{-2}$, $2\pi^{-1}3\pi^{-1}$, and $9\sigma^{-1}3\pi^{-1}$. That is, most of the types of electron configuration listed in Table I (except for σ^{-2}) are accessible. The observed β value (0.10) at 37 eV must be the result of competition between two types of transitions Σ-Σ and Σ-Π. If the cross section ($\sigma_\parallel$) for the Σ-Σ-type transitions is equal to that ($\sigma_\perp$) of Σ-Π, the β parameter is 0.5 from the equation [2]

$$\beta=\frac{2\sigma_\parallel-\sigma_\perp}{\sigma_\parallel+\sigma_\perp} \tag{4}$$

or the equivalent

$$\frac{\sigma_\parallel}{\sigma_\perp}=\frac{1+\beta}{2-\beta} . \tag{5}$$

Equation (5) gives $\sigma_\parallel/\sigma_\perp=0.58$ at 37 eV ($\beta=0.10$) and 0.84 at 50 eV ($\beta=0.37$), i.e., the Σ-Π-type transition ($\sigma_\perp$) is ~70% and ~20% more probable than the Σ-Σ-type transition ($\sigma_\parallel$) at 37 and 50 eV, respectively. The ground electronic state ($^3\Sigma^-$) does not dissociate [19,23]. If we assume that the cross sections for the two electronic states ($^3\Pi$ and $^1\Pi$) arising from the $9\sigma^{-1}3\pi^{-1}$ configuration are relatively small at 37 eV (this is because their lowest state is at about 35 eV [19], only 2 eV below the excitation energy), the main contributors to the dissociation $OC^+ + S^+$ at 37 eV are those arising from the configurations $3\pi^{-2}$ and $2\pi^{-1}3\pi^{-1}$. As can be seen in Table I, the total symmetry Π appears twice as often as the Σ symmetry for the configuration π^{-2}. If the cross sections for the individual Π channels equal one another and also equal that of the Σ channel, as a simple and rough approximation, $\sigma_\parallel/\sigma_\perp$ is 0.5, which results in $\beta=0$ (see the last column in Table I). It should be noted that the value β deduced from this approximation agrees with the observed one ($\beta=0.1$) within experimental error. Although the β parameter should be measured near the threshold for an experimental investigation of the total symmetries, it could not be measured for the reason mentioned in Sec. III.

The rise of the β parameter at higher energy (Fig. 5) may be due to the contribution of $\sigma^{-1}\pi^{-1}$ and σ^{-2} configurations. The lowest electronic state of these configurations is at about 35 and 41 eV ($9\sigma^{-2}$), respectively. From the simple consideration mentioned above with respect to the densities of the Σ and Π channels in the total symmetry for the $\sigma^{-1}\pi^{-1}$ and σ^{-2} configurations, the β parameter is 0.2 and 0.5, respectively. Although the assumption made here may be too simple, the observed trend of the β parameter follows this prediction.

The β parameters for other channels are shown in Fig. 6, in which only the mean values of those measured at the different angles are indicated. Three main aspects of the

TABLE I. Symmetry about dissociative double photoionization of OCS.

Electron configuration of OCS^{2+}	Symmetry of OCS^{2+} ion state	Dipole-allowed photoelectron $\Delta\lambda=0,\pm1$	Overlap-allowed photoelectron $\Delta\lambda=0$	Total symmetry	Asymmetry parameter β[a]
π^{-2}	Σ	σ	π	Π	
	Σ	π	π	Σ	0
	Σ	δ	π	Π	
	Δ	σ	π	Π	
	Δ	π	π	Σ	0
	Δ	δ	π	Π	
$\sigma^{-1}\pi^{-1}$	Π	σ	π	Σ	
	Π	π	π	Π	
	Π	σ	σ	Π	0.2
	Π	π	σ	Σ	
	Π	δ	σ	Π	
σ^{-2}	Σ	σ	σ	Σ	0.5
	Σ	π	σ	Π	

[a]Under the assumption that the cross sections for the individual Σ and Π channels of the total symmetry are the same.

β parameters in Fig. 6 are discussed. (1) The β parameter for each dissociation channel sometimes differs from the others beyond the uncertainty (typically $OC^+ + S^+$, $O^+ + S^+ + C$ or $C^+ + S^+ + O$, and $O^+ + CS^+$ at 50 eV). This is probably a natural consequence of the different ionic states involved in each dissociation channel. (2) The β parameters for the channels $O^+ + S^+ + C$ and $C^+ + S^+ + O$ are close to that for the case $\sigma_\parallel = \sigma_\perp$ ($\beta = 0.5$) around 50 eV and decrease at higher photon energies. Since the dissociation mechanism has not been elucidated for the three-body dissociation, particularly at higher energies, the meaning of the observed β parameter for these channels is less clear. Within the framework that linear fragmentation and a negligibly small amount of kinetic energy for the neutral fragment are still preserved at higher energies (this will be discussed later), the β parameter represents the sum of each β parameter of a given ionic state (plus photoelectrons) weighted by its transition probability and thus results from a net total symmetry. The β parameter is in the range of $0 < \beta < 0.65$ in Fig. 6, which yields $0.5\sigma_\perp < \sigma_\parallel < 1.2\sigma_\perp$. (3) In the region of the excitation energies of 80–100 eV, the observed β parameters for the channels $O^+ + S^+ + C$ and $C^+ + S^+ + O$ are close to zero, which means an isotropic distribution within the framework mentioned above. However, if the simple approximation is still applicable, the β parameter should be much larger than zero because the contribution of the $\sigma^{-1}\pi^{-1}$ and σ^{-2} configurations increases more and more at the higher excitation energies. One possibility is that the linear fragmentation with nearly zero kinetic energy of the neutral fragment is not preserved any more, and the simulation of the spectral profiles thus leads to a meaningless β parameter. However, when the dissociation of OCS^{2+} was examined by the triple coincidence PEPIPICO experiment at an excitation energy of 80 eV, the slope of the linear regression between t_1 (flight time of O^+) and t_2 (that of S^+), for the $O^+ + S^+ + C$ channel was near diagonal [24]. This means that the dissociation $O^+ + S^+ + C$ occurs instantaneously [12] and further suggests that most of the kinetic energy released in the Coulomb explosion is shared by the ionic fragments O^+ and S^+. In this case, the linear fragmentation is preserved as a good approximation, at least for the channel $O^+ + S^+ + C$. An obvious implication is that the cross sections for the transitions Σ-Π are larger than those of Σ-Σ at the higher excitation energies. At present, the energy dependence of the cross sections with respect to the Σ and Π total symmetries is not known to the best of our knowledge.

For the channel $C^+ + O^+ + S$, whether an anisotropy exists is not clear from the present results. For further elucidation of anisotropy in the direct dissociative double photoionization, at least the symmetry of ionic states involved in the transition should be defined by more laborious experiments such as triple coincidence (threshold electron-photoion-photoion).

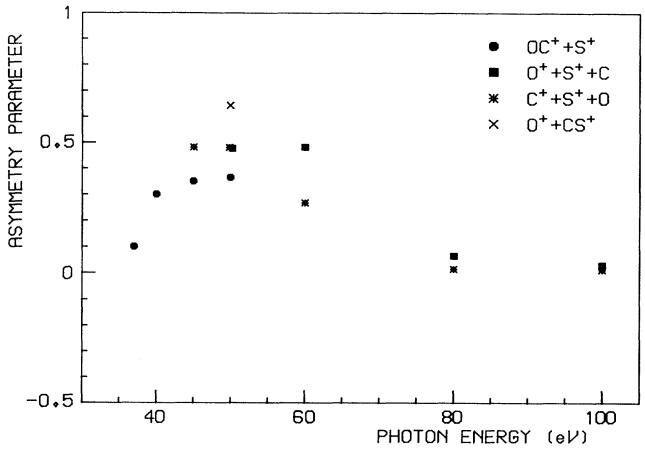

FIG. 6. Asymmetry parameter β for the channel $OC^+ + S^+$ (●), $O^+ + S^+ + C$ (■), $C^+ + S^+ + O$ (✱), and $O^+ + CS^+$ (×). For three-body dissociation, the β parameters strictly have meaning only in the limited dissociation mechanism in which the neutral is a spectator.

V. CONCLUSIONS

Angle-resolved photoion-photoion coincidence spectra have been measured for the direct double photoionization of the linear molecule OCS in the energy region of the valence orbitals by use of linearly polarized synchrotron radiation. The results indicate that clear anisotropies in fragmentation exist for most (four) of the observed five dissociation channels of OCS^{2+}. The present study shows that the anisotropy, observed here in the case of direct two-electron-ejection processes, can be understood in terms of the symmetry-characterized dissociation and the dynamics of the processes involved.

ACKNOWLEDGMENTS

The authors would like to thank the staff of the UVSOR facility of IMS for their invaluable help. They also wish to thank Professor H. Nakamura for many helpful discussions. This work was partially supported by Grant-in-Aid for Scientific Research No. 01540383 from the Ministry of Education, Science and Culture.

[1] R. N. Zare, Mol. Photochem. **4**, 1 (1972).
[2] J. L. Dehmer and D. Dill, Phys. Rev. A **18**, 164 (1978).
[3] N. Saito and I. H. Suzuki, Phys. Rev. Lett. **61**, 2740 (1988).
[4] A. Yagisita, H. Maezawa, M. Ukai, and E. Shigemasa, Phys. Rev. Lett. **62**, 36 (1989).
[5] N. Saito and I. H. Suzuki, J. Phys. B **22**, L517 (1989).
[6] N. Saito and I. H. Suzuki, Phys. Rev. A **43**, 3662 (1991).
[7] I. Powis, O. Dutuit, M. Richard-Viard, and P. M. Guyon, J. Chem. Phys. **92**, 1643 (1990).
[8] G. Dujardin, S. Leach, O. Dutuit, P. M. Guyon, and M. Richard-Viard, Chem. Phys. **88**, 339 (1984); G. Dujardin,

D. Winkoun, and S. Leach, Phys. Rev. A **31**, 3027 (1985); G. Dujardin, L. Hellner, D. Winkoun, and M. J. Besnard, Chem. Phys. **105**, 291 (1986).
[9] M. J. Besnowever, L. Hellner, G. Dujardin, and D. Winkoun, J. Chem. Phys. **88**, 1732 (1988).
[10] D. M. Curtis and J. H. D. Eland, Int. J. Mass Spectrom. Ion Phys. **63**, 241 (1985).
[11] J. H. D. Eland, F. S. Wort, and R. N. Royds, J. Electron Spectrosc. Relat. Phenom. **41**, 297 (1986).
[12] J. H. D. Eland, Mol. Phys. **61**, 725 (1987).
[13] T. Masuoka and I. Koyano, J. Chem. Phys. **95**, 909 (1991).
[14] S. Nagaoka, I. Koyano, and T. Masuoka, Phys. Scr. **41**, 472 (1990).
[15] T. Imamura, C. E. Brion, I. Koyano, T. Ibuki, and T. Masuoka, J. Chem. Phys. **94**, 4936 (1991).
[16] T. Masuoka, I. Koyano, and N. Saito (unpublished).
[17] T. Masuoka, T. Horigome, and I. Koyano, Rev. Sci. Instrum. **60**, 2179 (1989).
[18] E. Ishiguro, M. Suzui, J. Yamazaki, E. Nakamura, K. Sakai, O. Matsudo, N. Mizutani, K. Fukui, and M. Watanabe, Rev. Sci. Instrum. **60**, 2105 (1989).
[19] P. Millie, I. Nenner, P. Archirel, P. Lablanquie, P. Fournier, and J. H. D. Eland, J. Chem. Phys. **84**, 1259 (1986).
[20] See, for example, I. Nenner and J. A. Beswick, in *Handbook on Synchrotron Radiation, Vol. 2, Molecular Photodissociation and Photoionization,* edited by G. V. Marr (Elsevier, Amsterdam, 1987), p. 369.
[21] N. Saito and I. H. Suzuki, Int. J. Mass Spectrosc. Ion Proc. **82**, 61 (1988); J. Phys. B **22**, 3973 (1989); N. Saito, Denshi Gijutsu Sogo Kenkyusho Kenkyu Hokoku (Res. Rep. Comp. Res. Lab. Electron. Tech.) No. 910 (1990).
[22] P. Lablanquie, I. Nenner, J. H. D. Eland, J. Delwiche, M. J. Hubin-Franskin, and P. Morin, *Photophysics and Photochemistry above 6 eV,* edited by F. Lahmani (Elsevier, Amsterdam, 1985), p. 53.
[23] J. Ridard, B. Levy, and P. Millie, Chem. Phys. **122**, 403 (1988).
[24] T. Masuoka (unpublished data).